Results in Physics 8 (2018) 71–75

Contents lists available at ScienceDirect

Results in Physics

journal homepage: www.journals.elsevier.com/results-in-physics

Infiltration of MHD liquid into a deformable porous material

Anum Naseem [a], Asif Mahmood [b], J.I. Siddique [b,*], Lifeng Zhao [a]

[a] School of Mathematical Sciences, University of Science and Technology of China, Hefei, Anhui, China
[b] Department of Mathematics, Pennsylvania State University, York Campus, PA 17403, USA

ARTICLE INFO

Article history:
Received 19 May 2017
Received in revised form 11 October 2017
Accepted 31 October 2017
Available online 21 November 2017

ABSTRACT

We analyze the capillary rise dynamics for magnetohydrodynamics (MHD) fluid flow through deformable porous material in the presence of gravity effects. The modeling is performed using mixture theory approach and mathematical manipulation yields a nonlinear free boundary problem. Due to the capillary rise action, the pressure gradient in the liquid generates a stress gradient that results in the deformation of porous substrate. The capillary rise process for MHD fluid slows down as compared to Newtonian fluid case. Numerical solutions are obtained using a method of lines approach. The graphical results are presented for important physical parameters, and comparison is presented with Newtonian fluid case.

Introduction

Capillary rise is one of the most promising and vibrant illustrations of capillarity. This phenomena has been explored in various areas of science and engineering. Specially, it plays an important role in the lab-on-a-chip technologies, actuators and sensors, and fluid and thermal management devices to name a few [1,2]. The pioneering study in this area goes back to the Washburn model [3]. Washburn's study serves as a basis for further experimental as well as theoretical studies in rigid porous materials. In his experiment, he discussed the capillary rise phenomena by considering the porous material as a collection of cylindrical shape tubes. It was shown that in the absence of gravity, the capillary rise hight into rigid porous material in a time "t" is proportional to $\sqrt{t}$. His model has been used extensively to study capillary rise phenomena in rigid porous material. Many other studies that have taken into account the capillary rise phenomena into rigid porous material are [4–6].

The flow of liquid through deformable porous material has many applications in science and engineering including biomechanics, magma mechanics, ground water hydrology and soil consolidation [7]. Later on, Chen and Servin [8] performed an analysis to understand the flow in a deformable porous substrate. They noted that the passage of the fluid through a deformable porous material deforms the material which in turn influence the flow. The deformation in the porous material is because of forces associated with the flow of liquid. This suggests the need for such models that take into account both flow and deformation in porous material. The modeling approach that takes into account both fluid flow and liquid deformation is called the mixture theory. The main underlying idea of continuum mixture theory is that each constituent of the mixture is continuous and occupies every point in the space at each instant of time. Some of the studies that use mixture theory approach are [9–13]. More related work to our topic is the unidirectional infiltration under liquid pressure in an initially dry deformable porous medium by Sommer and Mortensen [14]. Their study showed a good agreement between the mathematical model and experiments. Preziosi et al. [15] explained the infiltration of an incompressible liquid in an initially dry, deformable sponge-like material where their theoretical predictions were backed up by experiments with reasonable agreement. Following the Preziosi work, Anderson [16] discussed a one-dimensional mathematical model describing the imbibition of liquid into deformable porous material. Later on, Siddique et al. [17] explained the capillarity and drainage phenomena under the effects of gravity of an incompressible fluid into a deformable porous material. They have presented a reasonable comparison between the theory and experiments describing the details linking with the classical work of Washburn [3], Lagon and Araujo [4] and Lockington and Parlange et al. [6].

The mechanism of magnetohydrodynamics is based upon the action of magnetic field on electrically conducting fluids. The applications of magnetohydrodynamics are in the geosciences, engineering, geophysics and medicine. In addition to these, magnetohydrodynamics fluids play an important role in electrostatic fibres, MHD accelerators, fluid droplets, cooling reactors, purification of crude oil and a lot many examples.

In this work we present a mathematical model for capillary rise of MHD liquid into deformable porous material under the effect of

* Corresponding author.
E-mail addresses: naseemanum@ymail.com (A. Naseem), aum54@psu.edu (A. Mahmood), jis15@psu.edu (J.I. Siddique), zhaolf@ustc.edu.cn (L. Zhao).

https://doi.org/10.1016/j.rinp.2017.10.059
2211-3797/

gravity. The mathematical model developed here is an analogue of the model taken by many authors [14–17] and helps in highlighting many important features due to the capillary rise of MHD liquid into deformable porous material. In the next section, we present the formulation of our mathematical model. In Section "R esults", we discuss the results via graphs. Finally, we conclude our discussion in the last section.

Modeling formulation

The magnetohydrodynamic flow of an incompressible fluid from liquid into a spongelike material is illustrated in Fig. 1. The surface of the material interacts with the liquid of an infinite stream at $z = 0$, and at time $t = 0$.

The liquid's upper surface is assumed to be open to the atmospheric pressure p_A. As time increases ($t > 0$), the liquid rises into the small pores of the material because of capillary suction under the assumption that the capillary pressure $p_c < 0$. This results in the deformation of the solid material. We denote the upper interface of the porous material by $h_\ell(t)$ and lower interface by $h_s(t)$. The other assumption is that the pressure in the fluid bath us hydrostatic i.e. $p = p_A - \rho_\ell g h_s$ at $z = h_s(t)$ along with the uniform initial solid volume fraction ϕ_0. Thus we are interested in the unknown variables in the deformed material under consideration and boundary positions h_s and h_ℓ, i.e., the velocity component of solid phase in the vertical direction w_s, the velocity component of liquid phase in the vertical direction w_ℓ, stress σ ($\sigma = \sigma I$) in the solid, pressure of the liquid p and solid volume fraction ϕ. A decent review of the literature [9,10,18] suggest the use of the mixture theory to model the problem of deformable porous media. The equation representing the conservation of mass for liquid constituents is given as

$$\frac{\partial \phi}{\partial t} - \frac{\partial}{\partial z}[(1-\phi)w_\ell] = 0, \tag{1}$$

where w_ℓ is velocity of liquid and $1 - \phi$ is liquid volume fraction. The equation representing the conservation of mass for solid phase is given as

$$\frac{\partial \phi}{\partial t} + \frac{\partial}{\partial z}(\phi w_s) = 0, \tag{2}$$

where w_s is velocity of solid and ϕ is solid volume fraction. The mathematical manipulation of momentum equations for liquid solid phases results into modified Darcy's law for imbibition of MHD liquid through deformable porous media

$$w_\ell - w_s = -\frac{K(\phi)}{(1-\phi)\mu}\left(\frac{\partial p}{\partial z} + \rho_l g\right) + \frac{K(\phi)\sigma_0 B_0^2}{(1-\phi)^2\mu} w_s, \tag{3}$$

where $K(\phi)$ is permeability of deformable porous material, μ is the dynamic viscosity, σ_0 is the electrical conductivity, B_0 denotes the uniform magnetic flux, g is the gravity and ρ_s and ρ_ℓ are actual intrinsic density of the solid and liquid, respectively. In the presence of gravity, the stress in the solid plus gravity and exertion of pressure due to liquid balance each other. In other words, neglecting inertial and body forces in both the solid and liquid phase, stress equilibrium states that

$$\frac{\partial p}{\partial z} = \frac{\partial \sigma}{\partial z} - g[\rho_s \phi + \rho_l(1-\phi)]. \tag{4}$$

here $\boldsymbol{\sigma}$, is component of stress tensor, p is the pressure, and z is the coordinate axis. Combining the two continuity equations yields, $\phi w_s + (1-\phi)w_\ell = c(t)$, where $c(t)$ is constant of integration. This relationship along with modified Darcy's law yields the following equations for solid and liquid velocities

$$w_s = \frac{(1-\phi)}{1-\phi+\alpha}\left\{c(t) + \frac{K(\phi)}{\mu}\left[\sigma'(\phi)\frac{\partial \phi}{\partial z} - g(\rho_s - \rho_l)\phi\right]\right\}, \tag{5}$$

$$w_\ell = \frac{c(t)}{1-\phi}\left[1 - \frac{\phi(1-\phi)}{1-\phi+\alpha}\right] - \frac{\phi}{1-\phi+\alpha}\frac{K(\phi)}{\mu}\left[\sigma'(\phi)\frac{\partial \phi}{\partial z} - g(\rho_s - \rho_l)\phi\right], \tag{6}$$

where $\alpha = \frac{K(\phi)\sigma_0 B_0^2}{\mu}$. Keeping in mind that α contains permeability $K(\phi)$, which will be replaced by its particular choice at the appropriate place. A simple mathematical manipulation of Eqs. (2), (4) and (5) result into a single partial differential equation for solid volume fraction ϕ in the wet region $h_s(t) \leqslant z \leqslant h_\ell(t)$

$$\frac{\partial \phi}{\partial t} + c(t)\frac{\partial}{\partial z}\left[\frac{\phi(1-\phi)}{1-\phi+\alpha}\right] = -\frac{\partial}{\partial z}\left[\frac{\phi(1-\phi)}{1-\phi+\alpha}\frac{K(\phi)}{\mu}\left\{\sigma'(\phi)\frac{\partial \phi}{\partial z} - g(\rho_s - \rho_l)\phi\right\}\right]. \tag{7}$$

A similar form of Eq. (7) is obtained by many authors [15–17] discussing their particular scenarios i.e. in the absence and presence of gravity effects. In our particular situation, we impose the

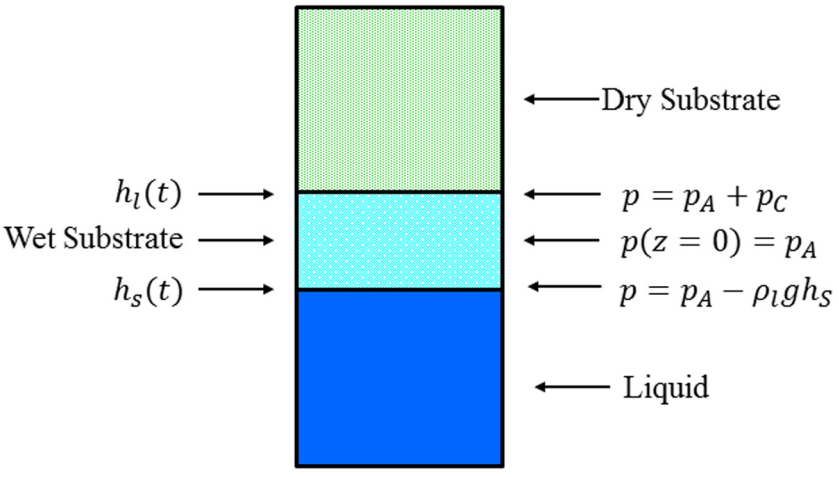

Fig. 1. Schematic diagram.

following kinematics, hydrostatic pressure assumption in the liquid phase and zero stress boundary conditions at solid boundary $z = h_s(t)$

$$w_s(h_s^+, t) = \frac{\partial h_s}{\partial t}, \tag{8}$$

$$p(h_s^+, t) = p_A - \rho_l g h_s(t), \tag{9}$$

$$\sigma(h_s^+, t) = 0, \tag{10}$$

where atmospheric pressure is represented by p_A. On similar lines, the kinematic and capillary pressure conditions at wet material-dry material interface $z = h_\ell(t)$ are

$$w_\ell(h_l^-, t) = \frac{\partial h_l}{\partial t}, \tag{11}$$

$$p(h_l^-, t) = p_A + p_c, \tag{12}$$

denoting capillary pressure by p_c. The determination of constant of integration $c(t)$ is performed following [15]

$$c(t) = \frac{\phi(1-\phi_0)(1-\phi)}{\alpha(\phi-\phi_0)-\phi_0(1-\phi)^2}\frac{K(\phi)}{\mu}\left[\sigma'\frac{\partial\phi}{\partial z} - g\phi(\rho_s-\rho_l)\right]. \tag{13}$$

One can combine Eqs. (5) and (6) with Eqs. (8) and (11) to get

$$\frac{\partial h_s}{\partial t} = \left[c(t)\frac{(1-\phi)}{1-\phi+\alpha} + \frac{K(\phi)}{\mu}\left\{\sigma'(\phi)\frac{\partial\phi}{\partial z} - g(\rho_s-\rho_l)\phi\right\}\frac{(1-\phi)}{1-\phi+\alpha}\right]_{h_s^+}, \tag{14}$$

$$\frac{\partial h_l}{\partial t} = \left[\frac{c(t)}{1-\phi}\left(1-\frac{\phi(1-\phi)}{1-\phi+\alpha}\right) - \frac{\phi}{1-\phi+\alpha}\frac{K(\phi)}{\mu}\left\{\sigma'(\phi)\frac{\partial\phi}{\partial z} - g(\rho_s-\rho_l)\phi\right\}\right]_{h_l^-}. \tag{15}$$

It is important to note that Eq. (7) represents solid volume fraction in the wet region and Eqs. (14) and (15) represent the interface positions for liquid and solid phases. In other words, (7) provides deformation in the solid locally and Eqs. (14) and (15) show deformation globally. In the following section, we present the procedure for non-dimemsionalization.

Non-dimensionalization and solution strategy

It is worth mentioning that Eq. (7) along with Eqs. (14) and (15) formulate a problem on a moving domain $h_s \leqslant z \leqslant h_\ell$. Solving a problem on a moving domain is a bit of a challenge. The first step that we initiate in this regard is to transform the problem to fixed domain by using the following transformation.

$$\bar{z} = \frac{z - h_s(t)}{h_l(t) - h_s(t)}, \quad \bar{t} = \frac{t}{T}.$$

In addition to the transformations listed above, we introduce the following choices of dimensionless quantities

$$\bar{h}_s = \frac{h_s}{L}, \quad \bar{h}_\ell = \frac{h_\ell}{L}, \quad \bar{p} = \frac{p}{m}, \tag{16}$$

which in turn yields the following scales for length $L = \frac{m}{\rho_l g}$ and time $T = \frac{L^2\mu}{mK_0}$. The forms of permeability $K(\phi)$ and stress $\sigma(\phi)$ that we will be using are $K(\phi) = \frac{K_0}{\phi}, K_0 > 0$ and $\sigma(\phi) = m(\phi_r - \phi), \sigma' = -m$. These choices are physically consistent with the realistic trend and are reasonable for a one dimensional case and need to be generalized for multidimensional cases. The above choice of stress is zero when the solid fraction is at constant relaxed value ϕ_r. Upon introducing the choices for dimensionless variables in Eq. (7), we obtain the following partial differential equation for ϕ,

$$\begin{aligned}
&\frac{\partial\phi}{\partial\bar{t}} + \left[\frac{\bar{z}-1}{\bar{h}_\ell-\bar{h}_s}\frac{d\bar{h}_s}{d\bar{t}} - \frac{\bar{z}}{\bar{h}_\ell-\bar{h}_s}\frac{d\bar{h}_\ell}{d\bar{t}}\right]\frac{\partial\phi}{\partial\bar{z}} \\
&+ \frac{\bar{c}(\bar{t})}{\bar{h}_\ell-\bar{h}_s}\left[\frac{\phi(1-2\phi)M}{(\phi-\phi^2+M)^2} + \frac{\phi(1-\phi)}{\phi-\phi^2+M}\right]\frac{\partial\phi}{\partial\bar{z}} \\
&= \frac{1}{\left(\bar{h}_\ell-\bar{h}_s\right)^2}\left[\frac{(1-2\phi)M}{(\phi-\phi^2+M)^2}\left(\frac{\partial\phi}{\partial\bar{z}}\right)^2 + \frac{\phi(1-\phi)}{\phi-\phi^2+M}\frac{\partial^2\phi}{\partial\bar{z}^2}\right] \\
&+ \frac{\rho}{\bar{h}_\ell-\bar{h}_s}\left[\frac{\phi(1-2\phi)M}{(\phi-\phi^2+M)^2} + \frac{\phi(1-\phi)}{\phi-\phi^2+M}\right]\frac{\partial\phi}{\partial\bar{z}}.
\end{aligned} \tag{17}$$

The next necessary ingredient for the above PDE are boundary conditions which we derive from zero stress condition (10) and stress equilibrium condition for solid volume fraction ϕ

$$\phi = \phi_r, \quad \text{at} \quad z = 0 \tag{18}$$

and we obtain the second boundary condition by integrating Eq. (4) and using the pressure boundary conditions (9) and (12)

$$\phi = \phi_l^* - \left(\bar{h}_l - \bar{h}_s\right)\int_0^1 (\rho\phi + 1)d\bar{z} - \bar{h}_s, \quad \text{at} \quad \bar{z} = 1, \tag{19}$$

where $\phi_l^* = \phi_r - \frac{p_c}{m}$. Finally, the dimensionless form of the constant function is

$$\bar{c}(\bar{t}) = -\left[\frac{\phi(1-\phi_0)(1-\phi)}{M(\phi-\phi_0)-\phi\phi_0(1-\phi)^2}\left[\frac{1}{\bar{h}_l-\bar{h}_s}\frac{\partial\phi}{\partial\bar{z}} + \rho\phi\right]\right]_{\bar{z}=1}. \tag{20}$$

The dimensionless forms of solid and liquid interface position upon introducing the dimensionless choices yields the following ODEs

$$\frac{d\bar{h}_s}{d\bar{t}} = \left[\frac{\bar{c}(\bar{t})\phi(1-\phi)}{\phi-\phi^2+M} - \frac{(1-\phi)}{\phi-\phi^2+M}\left[\frac{1}{\bar{h}_l-\bar{h}_s}\frac{\partial\phi}{\partial\bar{z}} + \rho\phi\right]\right]_{\bar{z}=0}, \tag{21}$$

$$\frac{d\bar{h}_l}{d\bar{t}} = \left[\frac{\bar{c}(\bar{t})}{(1-\phi)}\left[1 - \frac{\phi^2(1-\phi)}{\phi-\phi^2+M}\right] + \frac{\phi}{\phi-\phi^2+M}\left[\frac{1}{\bar{h}_l-\bar{h}_s}\frac{\partial\phi}{\partial\bar{z}} + \rho\phi\right]\right]_{\bar{z}=1}, \tag{22}$$

along with the following initial conditions for these interface positions

$$\bar{h}_l(\bar{t}=0) = 0, \quad \bar{h}_s(\bar{t}=0) = 0. \tag{23}$$

The above system of Eqs. (17)–(23) is solved numerically using the initial conditions $\phi(\bar{z}, \bar{t} = t_I) = \phi_s[\lambda_s + \bar{z}(\lambda_\ell - \lambda_s)]$ for PDE and $\bar{h}_s(\bar{t}_I) = 2\lambda_s\sqrt{\bar{t}_I}$ and $\bar{h}_\ell(\bar{t}_I) = 2\lambda_\ell\sqrt{\bar{t}_I}$ for the interface positions (see [17] for more details). The spatial derivatives are discretized using a second order finite difference scheme along with Matlab's ode15s solver for integration in time. The section below contains the outcome of these simulations.

Results

Fig. 2 shows the capillary rise dynamics $\bar{h}_\ell$ and solid deformation $\bar{h}_s$ interface positions for $M = 0$ and $M \neq 0$ in the presence of gravity effects. As we see from Fig. 2 that the capillary rise dynamics for both $M = 0$ and $M \neq 0$, initially start from the same point because both of them have the same initial condition and $M = 0.5$, shows slower dynamics until $t = 0.4$, shown by dashed line and ultimately reaches the same equilibrium position as $M = 0$ fluid shown by solid line. In contrast to this, the deformation in the solid material for $M = 0.5$ is much faster, shown by, a dashed line than $M = 0$ case. In summary, capillary rise dynamics for MHD

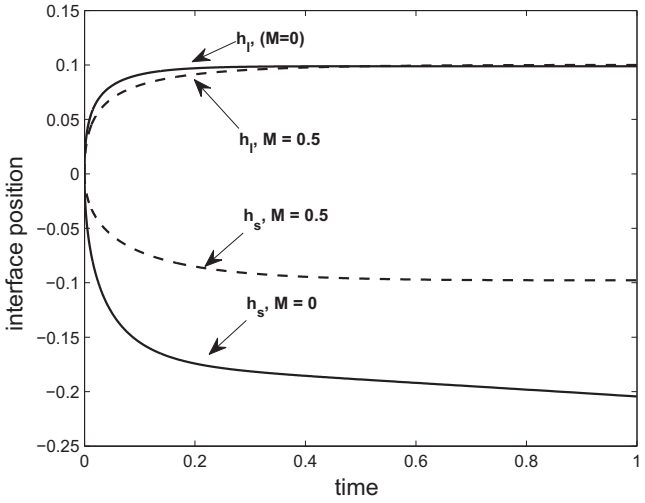

Fig. 2. The capillary rise dynamics h_ℓ and solid deformation h_s for $M = 0$ and $M \neq 0$ as a function of time. The other parameters value that we use are $\phi_0 = 0.33, \phi_r = 0.1, \phi_\ell = 0.20$ and $\rho = 0.1$.

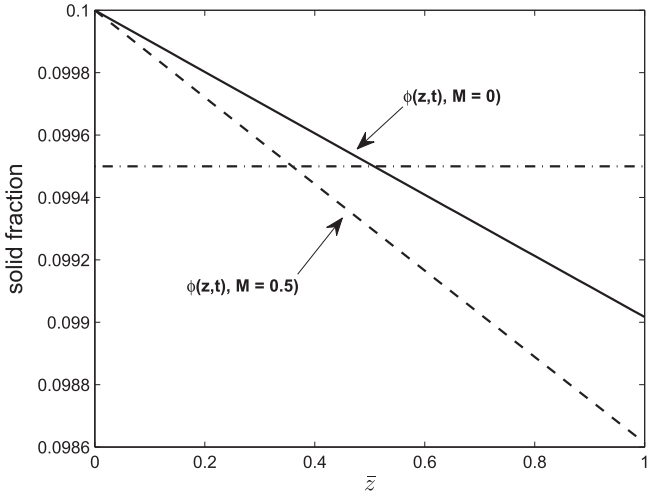

Fig. 4. Solid volume fraction unsteady $\phi(z,t)$ and steady ϕ as a function z for long time associated with the Fig. 4.

case reach equilibrium position whereas solid deformation dynamics is much faster than Newtonian fluid case.

Fig. 3 shows the capillary rise and solid deformation dynamics for the special choice of parameters when long time dynamics of solid deformation tends to zero. Interestingly, the deformable porous material shrinks initially which is represented by $h_s(t) > 0$. This is only possible if the liquid bath permanently remains in contact with the deformable solid material. The said behavior is associated with Newtonian liquid. Here we observe that the MHD fluid reach to an equilibrium height faster than the Newtonian liquid. For solid deformation for MHD liquid we observe that the solid material keeps deforming and reaches an equilibrium position different than $h_s = 0$. The Newtonian case for similar dynamics was also shown by Siddique et al. [17].

Fig. 4 shows the plot of solid volume fraction ϕ as function of z for unsteady Newtonian fluid shown by solid line and MHD liquid shown by dashed line cases. The comparison with analytically computed steady solution and numerically computed unsteady solution shows an excellent agreement which is not shown here.

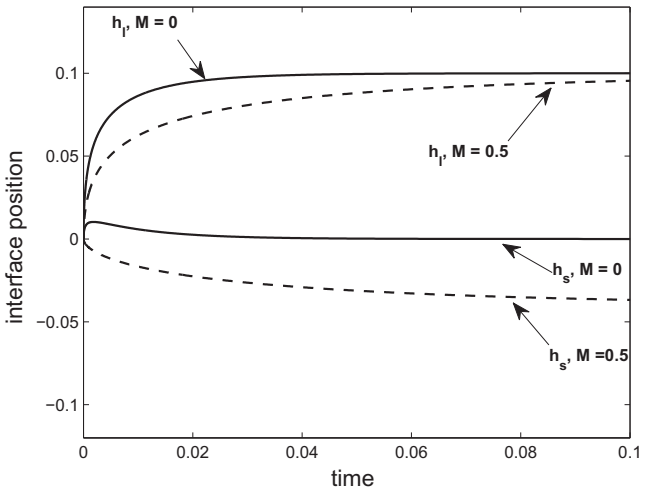

Fig. 3. Capillary rise dynamics h_ℓ and solid deformation h_s for $\phi_0 = 0.0995, \phi_r = 0.1, \phi_\ell = 0.20$ and $\rho = 0.1$.

These solutions are compared with constant solution ϕ_0, shown by the dashed line in the graph. Here we have used the same value of ϕ_0 so that $h_s = 0$. The two interesting phenomena that we wanted to observe are relative compression $\phi > \phi_0$, and relative expansion $\phi < \phi_0$. For positive values of ρ, the occurrence of local expansion happens near the top and local compression near the bottom. This process of local compression and expansion occurs in both MHD and Newtonian liquid and shows local deformation i.e. $h_s = 0$, which means zero net deformation.

This dynamics makes definite sense; when $\rho > 0$ the solid fraction decreases when we increase the spatial vertical position for MHD liquid. On the other hand, when $\rho < 0$, the opposite trend is observed. For the case of $\rho = 0$, we obtain $\phi = \phi_r$ for both Newtonian and MHD liquid. These observations are physically consistent. As for the case $\rho_s > \rho_\ell$, the solid material accumulation of MHD liquid near the bottom is quicker than Newtonian liquid, and when $\rho_\ell > \rho_s$, the liquid accumulation near the bottom is quicker for MHD liquid as compared to Newtonian liquid.

Conclusion

In this his article we studied the capillary rise of MHD liquid into deformable porous material. The new contribution in this research is changing the Newtonian liquid to MHD liquid. Evidently, the resulting system of equations are relatively difficult and add on interesting physics in capillary rise phenomena.

For the MHD fluid case, the liquid interface position reached the same steady state position whereas the solid interface for the MHD liquid reached to the steady state position before Newtonian liquid and is expected to get to the same interface position if we run the numerical simulation for long enough time. On the similar lines, for the special choice of parameters that yields $h_s = 0$, the solid interface position keeps deforming and ultimately reaches a steady state height. Similar dynamics is observed in Fig. 3, where unsteady Newtonian and MHD fluid cases for $t \to \infty$ are plotted as a function of z. The accumulation of solid material for Newtonian and MHD liquid is seen for both $\rho_s > \rho_\ell$ and $\rho_\ell > \rho_s$ cases.

The MHD capillary rise dynamics for one dimensional deformable porous materials shows many interesting features that need experimental justifications and further analysis of the model for higher dimensions. Analysis of the full nonlinear moving boundary value problem along with the inclusion of different permeability functions are the topics of further research.

Acknowledgments

This material is based on work supported by the Simons Foundation grant number 281839^3 and Penn State York^{2,3}.

Appendix A. Supplementary data

Supplementary data associated with this article can be found, in the online version, athttps://doi.org/10.1016/j.rinp.2017.10.059.

References

[1] De Gennes PG. Wetting: statics and dynamics. Rev Mod Phys 1985;57:827863.
[2] Darhuber AA, Troian SM. Principles of microfluidic actuation by modulation of surface stresses. Annu Rev Fluid Mech 2005;37:425–55.
[3] Washburn EW. The dynamics of capillary flow. Phys Rev 1921;17:273.
[4] Lago M, Araujo M. Capillary rise in porous media. J Colloid Interface Sci 2001;234:35–43.
[5] Zhmud BV, Tiberg F, Hallstensson K. Dynamic of capillary rise. J Colloid Interface Sci 2000;228:263–9.
[6] Lockington DA, Parlange J-Y. A new equation for macroscopic description of capillary rise in porous media. J Colloid Interface Sci 2004;278:404.
[7] Biot MA. General theory of three-dimensional consolidation. J Appl Phys 1941;12:155.
[8] Chen KSA, Scriven LE. Liquid penetration into a deformable porous substrate. Tappi J 1990;73:151.
[9] Bowen MR. Incompressible porous media models by use of the theory of mixtures. Int J Eng Sci 1980;18:1129.
[10] Atkin RJ, Crain RE. Continuum theories of mixture: basic theory and historical development, Q.J. Mech. Appl Math 1976;29:209.
[11] Hou JS, Holmes MH, Lai WM, Mow VC. Boundary conditions at the cartilage-synovial fluid interface for joint lubrication and theoretical verifications. J Biomech Eng 1989;111:78.
[12] Barry SI, Aldis GK. Radial flow through deformable porous shells. J Aust Math Soc Ser B Appl Math 1993;34:333.
[13] Barry SI, Aldis GK. Flow induced deformation from pressurized cavities in absorbing porous tissues. Bull Math Biol 1992;54:977.
[14] Sommer JL, Mortensen A. Forced unidirectional infiltration of deformable porous media. J Fluid Mech 1996;311:193.
[15] Preziosi L, Joseph DD, Beavers GS. Infiltration of initially dry, deformable porous media. Int J Multiphase Flow 1996;22:1205.
[16] Anderson DM. Imbibition of a liquid droplet on a deformable porous substrate. Phys Fluids 2005;17:087104.
[17] Siddiqui JI, Anderson DM, Bondarev A. Capillary rise of a liquid into a deformable porous material. Phys Fluids 2009;21:013106.
[18] Rajagopal KR, Tao L. Mechanics of mixtures, 1995.